13A.3   ASSIMILATION OF POLARIMETRIC RADAR DATA USING
ENSEMBLE KALMAN FILTER: EXPERIMENT WITH SIMULATED DATA

Youngsun Jung[1,2,*], Ming Xue[1,2], and Jerry M. Straka[1]
[1]School of Meteorology and [2]Center for Analysis and Prediction of Storms
University of Oklahoma, Norman OK 73019

1. Introduction

Since the use of differential reflectivity for rainfall estimation was first proposed by Seliga and Bringi (1976), many studies have shown that polarimetric measurements can improve precipitation type classification and quantitative precipitation estimate (Straka et al. 2000). Moreover, the polarimetric radar (PR) upgrade plan of the National Weather Services (NWS) for the operational WSR-88D network radars will undoubtedly motivate more active research on the utilization of PR data.

A more accurate estimate of the amounts of hydrometeors using PR data can contribute to the improvement and verification of microphysical parameterizations in cloud and mesoscale models. It can provide a useful means for the initialization of hydrometeor types and amount for storm-scale and mesoscale NWP models, and help the verification of quantitative precipitation forecasts (QPF). Such estimations can also help enhance our understanding of the interactions between microphysics and kinematics in severe storms and mesoscale system (Straka et al. 2000). Polarimetric radars also should be helpful for storm-scale model initialization through data assimilation.

Initialization of convective storms using radar data within a numerical model has enjoyed reasonable success in recent years, using methods such as the complex cloud analysis, 4DVAR and more recently the ensemble Kalman filter (EnKF). The first paper which investigates the potential of EnKF to assimilate Doppler radar data into cloud model with a warm rain microphysics only is Snyder and Zhang (2003). In their study, state variables not directly observed are successfully retrieved using EnKF. The recent studies of Tong and Xue (2005, TX05 hereafter) and Xue et al. (2005, hereafter XTD05) also show that the cloud fields, including microphysical species associated with a 3-ice microphysics scheme, can be accurately retrieved using the EnKF method from simulated radial velocity and reflectivity data.

It is expected that the analysis results can be further

improved when additional polarimetric parameters are assimilated. The parameters include differential reflectivity (Z_{dr}), specific differential phase (K_{dp}) and possibly some other parameters for hydrometeor classification. Wu et al. (2000) used Z_{dr} indirectly in a cloud-scale 4DVAR data assimilation system; the reflectivity (Z) and differential reflectivity were first converted to rain and ice mixing ratios which are subsequently assimilated together with the radial velocity (V_r) data.

In this study, the direct assimilation of dual polarization radar data using an ensemble Kalman filter is explored for the first time. Forward observation operators for the polarimetric radar measurements that are consistent with microphysics schemes with varying degrees of assumptions are first developed and their sensitivities to the assumptions are examined. These observational operators are then used to create simulated data sets from a model storm, and the impacts of these data are examined through Observing System Simulation Experiments (OSSEs).

2. Description of assimilation experiments

a. The assimilation scheme and prediction model

The particular variant of ensemble Kalman filter used in this study is the ensemble square-root filter (EnSRF) after Whitaker and Hamill (2002). The OSSE framework used in this study is described in detail by XTD05. The physical domain used for the experiments is $66 \times 66 \times 16$ km^3 with a horizontal spacing of 1.5 km and a vertically stretched grid with a minimum grid spacing of 100m near the surface. The Advanced Regional Prediction System (ARPS) is used in both simulation and analysis and is documented in Xue et al. (2000; 2001; 2003).

The truth simulation is initialized in the same way as for the slow-moving system in the small domain of XTD05. The environmental sounding used to for the truth simulation is that of the 20 May 1977 Del City, Oklahoma supercell storm. Our experiments are an extension of experiment named TLX described in XTD05, with the addition of polarimetric data measurements.

b. Observation operators

The set of forward observation operators that link the

---

* *Corresponding author address*: Youngsun Jung, School of Meteorology, University of Oklahoma, Norman OK 73019.
E-mail: youngsun.jung@ou.edu

dual polarization measurements with the model state variables are first developed and efforts are made to ensure their consistency with the ARPS 3-ice microphysics scheme based on Lin et al. (1983). These observation operators are then incorporated into our EnSRF system to assimilate the corresponding polarimetric parameters.

The equivalent reflectivity of raindrops for horizontal and vertical polarizations are, based on Zhang et al. (2001), respectively,

$$Z_{rh} = \frac{4\lambda^4 \alpha_a^2 n_0}{\pi^4 |K_w|^2} \Lambda^{-(2\beta_a+1)} \Gamma(2\beta_a+1) \qquad (1)$$

$$Z_{rv} = \frac{4\lambda^4 \alpha_b^2 n_0}{\pi^4 |K_w|^2} \Lambda^{-(2\beta_b+1)} \Gamma(2\beta_b+1) \qquad (2)$$

where λ = 10.7 cm is the wavelength, that of the WSR-88D radars, $n_0 = 8\times10^6$ m^{-4} is the intercept parameter of the exponential drop size distribution, $K_w = 0.93$ is the dielectric factor for water, and $\alpha_a = 4.26\times10^{-4}$, $\alpha_b = 4.76\times10^{-4}$, $\beta_a = 3.02$, and $\beta_b = 2.69$ are non-dimensional coefficients.

For dry snow, the equivalent reflectivity equation given below following Ryzhkov et al. (1998) replaces Eq. (5) of TX05:

$$Z_{s,dry} = \frac{a_1}{9|K_w|^2} \frac{\Gamma(2\delta+1)}{\Gamma(\delta+1)} \gamma^2 D_{ns}^{2\delta+1} n_s \Gamma(\delta+1), \qquad (3)$$

where $a_1 = 7.3$, $\delta = 1.9$, $\gamma = 0.0117\pi$, $n_s = 4\times10^4$ m^{-4}. D_{ns} is the characteristic diameter defined as the inverse of slope parameter Λ. In this formula, the density of snow is a function of size (Locatelli and Hobbs 1974), so it is not exactly consistent with the ARPS microphysics that assumes a single density for snow. This formula gives significantly smaller reflectivity values at high altitudes where most ice crystals are small. In the future, we will seek to upgrade the ARPS microphysics for the snow density to depend on particle diameter. The formulas for wet snow and dry and wet hail are the same as those given in TX05.

Those equivalent reflectivities for different species are combined to give differential reflectivity

$$Z_{dr} = 10\log_{10}\left(\frac{Z_{hh}}{Z_{vv}}\right) = 10\log_{10}\left(\frac{Z_{rh}+Z_s+Z_h}{Z_{rv}+Z_s+Z_h}\right). \qquad (4)$$

Here, Z_{hh} and Z_{vv} are the reflectivities at horizontal and vertical polarization, respectively. The first subscript r, and single subscript s and h denote rainwater, snow and hail, respectively. An example of simulated Z and Z_{dr} at the 1.5 km altitude at 90 minutes of truth storm is presented in Fig. 1. We show the 1.5-km level because Z_{dr} is usually greater at lower altitudes where the hydrometeors are mostly raindrops. In contract to the reflectivity field, Z_{dr} shows two minima near the center of domain

and at around $x = -18$ and $y = 14$ km, where the reflectivities are at a maximum. These maxima are due to high concentration of hail in these precipitation cores, where the associated Z_{dr} is weak; this behavior is consistent with our Z_{dr} formulation (4).
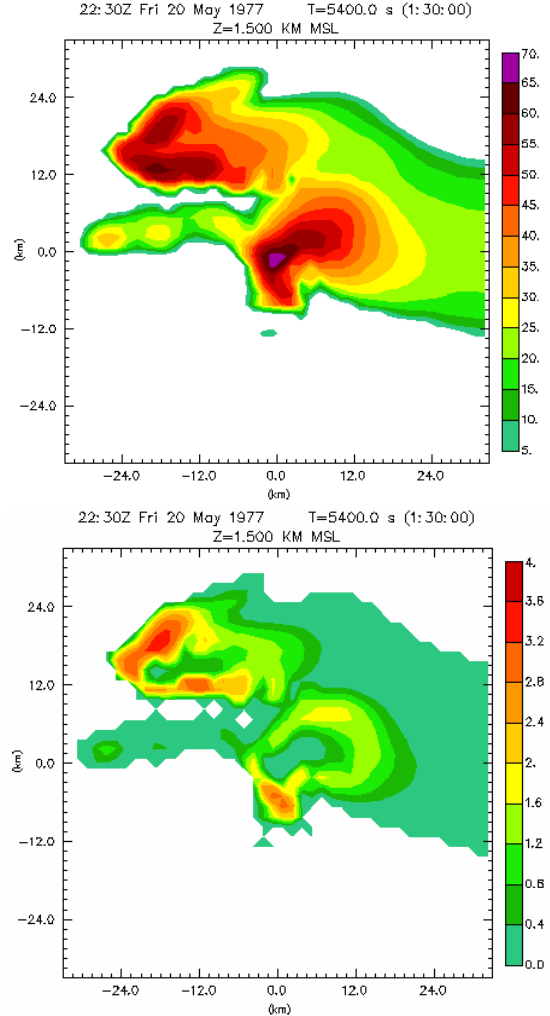

Fig. 1. The reflectivity at horizontal polarization Z (upper panel) and differential reflectivity Z_{dr} (lower panel) at 1.5 km altitude at 90 min of truth storm.

c. The experiment design

As in XTD05, initial ensemble members are initialized at t=20 min of model time by adding random perturbations of Gaussian distribution to the initially horizontal homogeneous first guess defined by a sounding. The pressure and microphysical variables are not perturbed.

The first assimilation of simulated observations is performed at 25 min of model time and the analyses are repeated every 5 min until 100 min. The filter uses 40 ensemble members. A single WSR-88D radar that scans

the model atmosphere is located to the northeast at about 90 km from the center of model grid.

We examine in particular the impact of assimilating differential reflectivity (Z_{dr}) and reflectivity at vertical polarization (Z_{vv}), in addition to radial velocity (V_r) and reflectivity at horizontal polarization (Z_{hh}), on the analysis and prediction of the thunderstorm. It is assumed that Z_{dr} is only available where its value is equal to or greater than 0 dB. Thus, Z_{dr} is assimilated only where its value is greater than 0 dB. Z_{vv} is assimilated only where Z_{hh} is greater then 10 dBZ to save computation while Z_{hh} data within the entire radar range are assimilated. For more detailed information on the configuration of the assimilation experiment, the reader is referred to XTD05.

d. Observations

A Gaussian power-gain weighting function described in XTD05 is also used to simulate Z_{hh}, Z_{vv}, and V_r observations on the radar elevation planes from the gridded fields of the truth simulation. Operational polarimetric WSR-88D radars will measure Z_{hh} and Z_{vv} from the same pulses. As a result, some of the errors in Z_{hh} and Z_{vv} should be correlated, which should reduce the error in Z_{dr} because Z_{dr} is related to the ratio of Z_{hh} and Z_{vv}. We therefore model the errors in Z_{hh} and Z_{vv} using

$$Z_{hh}^o = Z_{hh}^t + \varepsilon_c + \varepsilon_h,$$
$$Z_{vv}^o = Z_{vv}^t + \varepsilon_c + \varepsilon_v, \tag{5}$$

where superscripts t and o denote the truth and simulated observation, respectively. ε_c represents the correlated part of error and ε_h and ε_v are uncorrelated errors for Z_{hh} and Z_{vv}, respectively. For example, random errors ε_c and ε_h (and ε_v) are independently sampled from Gaussian distributions of zero mean and standard deviations of 3.0 dBZ and 0.22 dBZ, respectively and added to the truth. This set of errors results in Z_{hh} error of about 2.2 dBZ and Z_{dr} error of about 0.2 dB when calculated for the data collected over the entire domain for the entire assimilation times in terms of standard deviation. The errors of vertically polarized reflectivity are treated in a similar way. These error sizes should be valid for well-calibrated radars (A. Ryzhkov, personal communication, 2005). Standard deviation of V_r error is assumed to be 2 ms^{-1}. The standard deviations of errors assumed for Z and V_r are 5 dBZ and 1 ms^{-1}, respectively, in XTD05 and TX05.

3. Results

Out of curiosity, we first tried assimilating Z_{dr} data alone, without radial velocity or regular reflectivity data. The results of analysis were poor (not shown). This is not surprising because Z_{dr} mainly carries the information on the difference between reflectivities of horizontal and vertical polarization; it does not provide much information on the magnitude of the reflectivity, and is therefore by itself not able to analyze the mixing ratios of cloud and hydrometeor fields. However, as will be shown, Z_{dr} has a positive impact on analysis when combined with reflectivity and radial velocity data.

We further examined the impact of assimilating both Z_{hh} and Z_{vv}. It is found that assimilating Z_{vv} in addition to Z_{hh} and V_r has almost no impact with the standard deviations of observational errors specified earlier (not shown). The impact of assimilating Z_{vv} when the errors in Z_{hh} and V_r are increased will be explored further in a later study.

Fig. 2 shows the root-mean-square (rms) error curves for each model state variable during the assimilation period. It can be seen that assimilating additional polarimetric measurement, Z_{dr}, improves the analyses. Improvement mostly dramatic in rain water mixing ratio, q_r, as the corresponding black curves show lower errors. The vertical profiles of rms errors at the end of the assimilation cycle, i.e., at 100 min, are plotted in Fig. 3. It is seen that the errors in vertical velocity are decreased at all levels by assimilating Z_{dr} among the wind fields. Again, the reduction of error is largest for q_r. This is reasonable because Z_{dr} is most strongly tied to raindrops.

It should be noted that because the analysis using V_r and Z_{hh} was already very good, there is not too much room for further improvement, within the current OSSE framework with the perfect model assumption. For real data cases where model errors and data quality problems do exist, the extra information content afforded by the polarimetric data is expected to produce larger impact. This will be examined in the future.

We have also examined the sensitivity of analysis to observational operators with larger reflectivity error. We performed the experiment in which the reflectivity observations are generated using the formulas in XTD05 while the assimilation is performed using the equations presented in this paper and vice versa. The results show that EnSRF is not sensitive to the differences between these two sets of observation operators when V_r is assimilated along with Z_{hh}. When Z_{hh} is assimilated alone, the difference in q_s field is noticeable (not shown). This agrees with the discussion in section 2b. We will revisit this issue when considering the cases where more uncertainties in the observational operators and/or when the prediction model errors are present.

4. Summary and discussion

In this study, we extended our ensemble square-root Kalman filter to assimilate, in addition to regular reflec-

tivity and radial velocity, the simulated differential reflectivity and the reflectivity at vertical polarization, for a supercell storm. It is found that the assimilation of Z_{dr}, in addition to conventional reflectivity and radial velocity, improves the analysis, and among the state variables, the positive impact is largest for q_r. A positive impact can be seen in w even though it is not very significant.

Future work will include the assimilation of additional parameters such as specific differential phase. Due to the lack of the relationships between polarimetric variables except for Z_{dr} and different types of hydrometeors including raindrops, hail, graupel, snow and crystals, new formulas may need to be derived. One possible approach is to use radar scattering models and T-matrix method to derive the relationships. These observation operators will also be refined based on observational evidences and for them to be coupled with more sophisticated microphysics.

For shorter wavelength radars, such as the X-band radars to be installed by the new NSF Engineering Research Center for Collaborative Adaptive Sensing of the Atmosphere (CASA), the project that supports the current work, attenuation is an issue that has to be dealt with. An appropriate attenuation correction for the polarimetric measurements needs to be built into the observation operators and/or applied to the data. We hope the additional polarimetric radar measurements to be helpful for improving attenuation correction also, as it helps to improve the analysis of hydrometeor contents. Future studies will also include an assessment of the ability of our assimilation system for quantitative precipitation estimation (QPE).

Acknowledgement

References

Lin, Y.-L., R. D. Farley, and H. D. Orville, 1983: Bulk parameterization of the snow field in a cloud model. *J. Climate Appl. Meteor.*, **22,** 1065-1092.

Locatelli, J. D. and P. V. Hobbs, 1974: Fall speeds and masses of solid precipitation particles. *J. Geophys. Res.*, **79,** 2185-2197.

Ryzhkov, A. V., D. S. Zrnic, and B. A. Gordon, 1998: Polarimetric method for ice water content determination. *J. Appl. Meteor.*, **37,** 125-134.

Seliga, T. A. and V. N. Bringi, 1976: Potential use of radar differential reflectivity measurements at orthogonal polarizations for measuring precipitation. *J. Appl. Meteor.*, **15,** 59-76.

Snyder, C. and F. Zhang, 2003: Assimilation of simulated Doppler radar observations with an ensemble Kalman filter. *Mon. Wea. Rev.*, **131,** 1663-1677.

Straka, J. M., D. S. Zrnic, and A. V. Ryzhkov, 2000: Bulk hydrometeor classification and quantification using polarimetric radar data: Synthesis of relations. *J. Appl. Meteor.*, **39,** 1341-1372.

Tong, M. and M. Xue, 2005: Ensemble Kalman filter assimilation of Doppler radar data with a compressible nonhydrostatic model: OSS Experiments. *Mon. Wea. Rev.*, 1789-1807.

Whitaker, J. S. and T. M. Hamill, 2002: Ensemble data assimilation without perturbed observations. *Mon. Wea. Rev.*, **130,** 1913-1924.

Wu, B., J. Verlinde, and J. Sun, 2000: Dynamical and microphysical retrievals from Doppler radar observations of a deep convective cloud. *J. Atmos. Sci.*, **57,** 262-283.

Xue, M., K. K. Droegemeier, and V. Wong, 2000: The Advanced Regional Prediction System (ARPS) - A multiscale nonhydrostatic atmospheric simulation and prediction tool. Part I: Model dynamics and verification. *Meteor. Atmos. Physics*, **75,** 161-193.

Xue, M., M. Tong, and K. K. Droegemeier, 2005: An OSSE framework based on the ensemble square-root Kalman filter for evaluating impact of data from radar networks on thunderstorm analysis and forecast. *J. Atmos. Ocean Tech.*, Accepted.

Xue, M., D.-H. Wang, J.-D. Gao, K. Brewster, and K. K. Droegemeier, 2003: The Advanced Regional Prediction System (ARPS), storm-scale numerical weather prediction and data assimilation. *Meteor. Atmos. Physics*, **82,** 139-170.

Xue, M., K. K. Droegemeier, V. Wong, A. Shapiro, K. Brewster, F. Carr, D. Weber, Y. Liu, and D.-H. Wang, 2001: The Advanced Regional Prediction System (ARPS) - A multiscale nonhydrostatic atmospheric simulation and prediction tool. Part II: Model physics and applications. *Meteor. Atmos. Phy.*, **76,** 143-165.

Zhang, G., J. Vivekanandan, and E. Brandes, 2001: A method for estimating rain rate and drop size distribution from polarimetric radar measurement. *IEEE Trans. Geosci. Remote Sens.*, **39.**
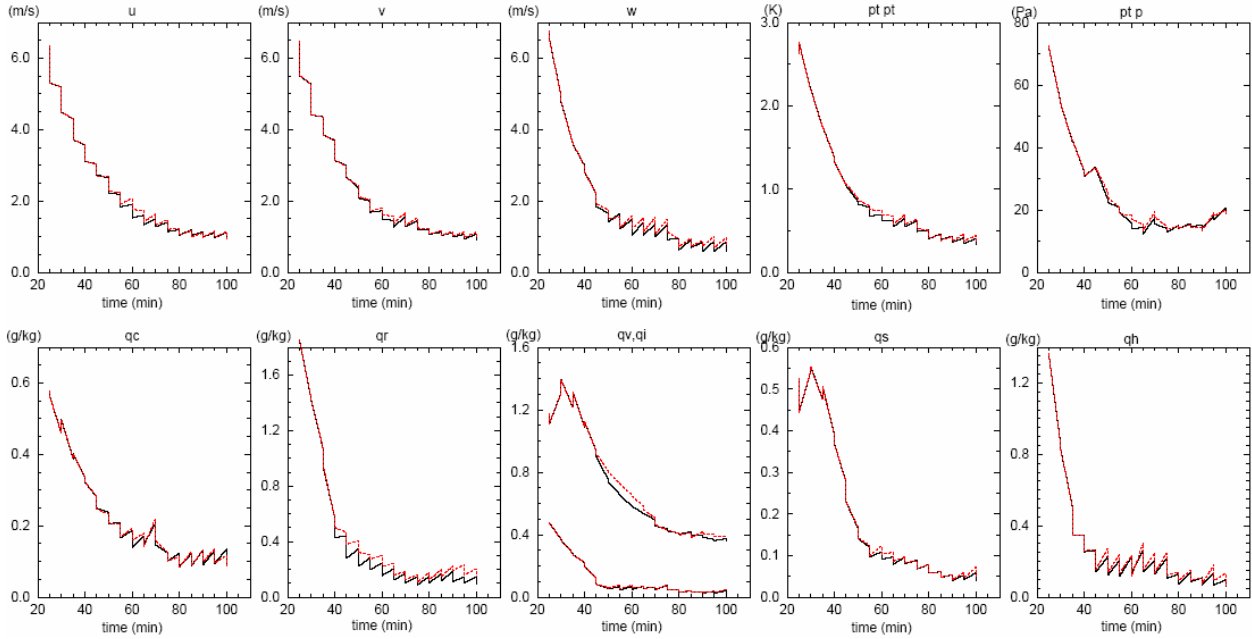
Fig. 2. The rms errors of ensemble-mean forecast and analysis, averaged over points at which the reflectivity is greater than 10 dBZ for: a) u, b) v, c) w and d) perturbation potential temperature θ', e) perturbation pressure p', f) cloud water q_c, g) rainwater q_r, h) water vapor q_v (the curves with larger values), cloud ice q_i (the curves with lower values), i) snow q_s, and j) hail q_h, for the experiment that uses V_r and Z only (red dashed), and the experiment that assimilates in addition Z_{dr} (thin black). The drop of the error curves at specific times corresponds to the reduction of forecast errors by analysis.
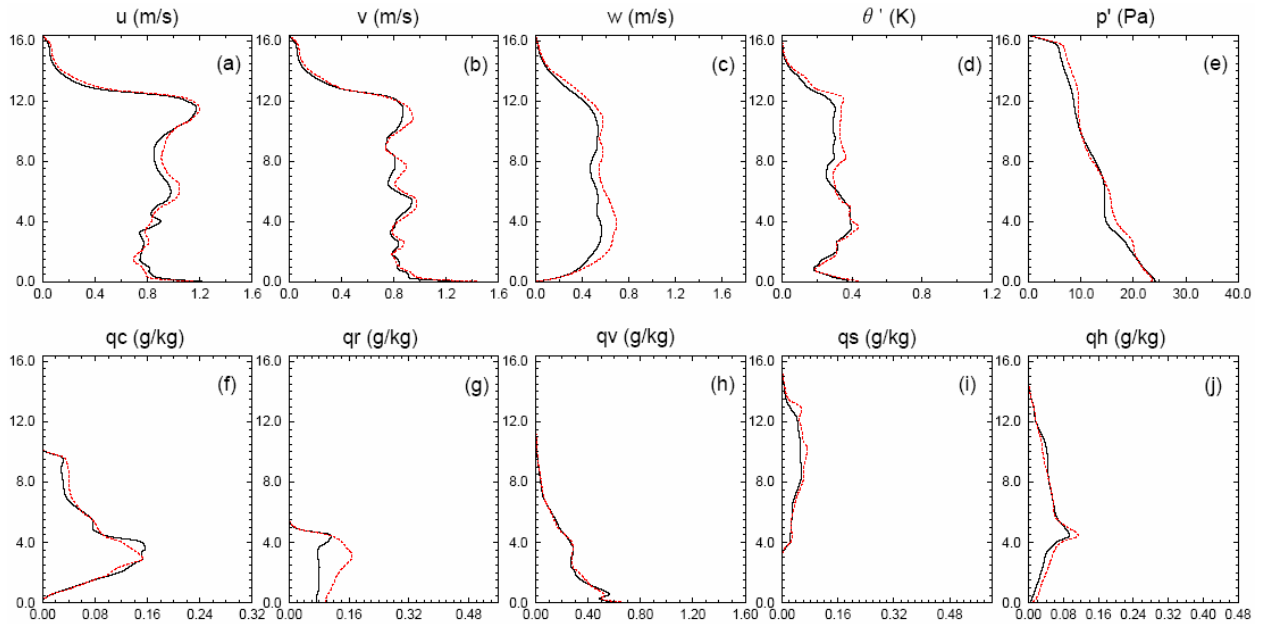

Fig. 3. The vertical profile of rms errors of EnSRF analysis at 100 min averaged over the entire horizontal domain for: a) u, b) v, c) w, d) θ', e) p', f) q_c, g) q_r, h) q_v, i) q_s, and j) q_h, for the experiment that uses V_r and Z only (red dashed), and the experiment that assimilates Z_{dr} (thin black).